Int. J. Electrochem. Sci., 14 **(2019)** 8161 – 8172, doi: 10.20964/2019.08.56

International Journal of ELECTROCHEMICAL SCIENCE
www.electrochemsci.org

Electrochemical Performance of $LiNi_{0.5-x}Zr_xMn_{1.5}O_4$(x= 0.00, 0.03, 0.05, 0.10) cathode materials for Lithium-ion Batteries

Shaoping Feng[1,2], Xin Kong[1,2], Hongyan Sun[1,2], Feihe He[3], Guowei Zhang[1,2], Wei Li[1,2], Baosen Wang[1,2], Yulai Duan[1,2], Guiyang Liu[1,2,]*

[1] Department of Chemistry, College of Science, Honghe University, Mengzi, 661199, Yunnan, China
[2] Local Characteristic Resource Utilization and New Materials Key Laboratory of Universities in Yunnan, Honghe University, Mengzi, 661199, Yunnan, China.
[3] Yunnan Copper Co., Ltd. Kunming, 650000, Yunnan, China.
[*]E-mail: liuguiyang@tsinghua.org.cn

Received: 8 March 2019 / *Accepted:* 20 May 2019 / *Published:* 10 June 2019

$LiNi_{0.5-x}Zr_xMn_{1.5}O_4$(x= 0.00, 0.03, 0.05, 0.10) were prepared by a combustion synthesis method. The results of X-ray diffraction (XRD) and Fourier transform infrared spectroscopy (FT-IR) reveal that the as-synthesized $LiNi_{0.5-x}Zr_xMn_{1.5}O_4$(x=0.00, 0.03, 0.05, 0.10) samples predominantly exist as ordered $P4_332$ space group and the second phase ZrO_2 appears when the Zr content reaches 0.05. Scanning electron microscopy (SEM) shows that the samples with different Zr content present porous morphology and have less particle sizes than the bare sample of $LiNi_{0.5}Mn_{1.5}O_4$. The electrochemical performances of $LiNi_{0.5-x}Zr_xMn_{1.5}O_4$(x=0.00, 0.03, 0.05, 0.10) samples suggest that the cycle performance and rate capability both at 25°C and 55°C are significantly improved after Zr modifying.

Keywords: $LiNi_{0.5}Mn_{1.5}O_4$, Electrochemical performance, Rate capability, Lithium-ion batteries

1. INTRODUCTION

$LiNi_{0.5}Mn_{1.5}O_4$ (LNMO) is considered to be a potential candidate for lithium-ion batteries (LIBs) because of its high energy density, high voltage (4.7V), environment-friendly and low cost [1, 2]. However, LNMO still suffers from severe capacity fade and poor cycling stability, especially at elevated temperature [3]. Several strategies such as morphology control [4, 5], surface coating [6, 7] and element doping [8, 9] have been employed to solve above-mentioned problems. Among them, it is the element doping that is usually used to improve the electrochemical performances of LNMO. Many modified LNMO with different doping elements, including Na[10], Cu[11], Zn[12], Al[13], Co[14], Cr[15], Si[16], Sm[17], Ru[18] and Nb[19] exhibited improved electrochemical performances.

Yoon et al.[20] revealed that Zr-doped $LiNi_{0.5}Mn_{1.5}O_{4-\delta}$ can provide more reversible structural

changes than the undoped LNMO, resulting in excellent cycling stability. We found that the ordered Zr-doped LNMO ($LiNi_{0.5}Mn_{1.49}Zr_{0.01}O_4$) exhibited significantly improved cycling stability and rate capability, while disordered LNMO changes little after Zr doping in our previous study [21]. Therefore, Zr doping should be a powerful way to enhance the electrochemical performances of LNMO. In order to explore the influence of Zr content on LNMO, $LiNi_{0.5-x}Zr_xMn_{1.5}O_4$(x=0.00, 0.03, 0.05, 0.10) were synthesized and their electrochemical performances were studied in detail.

2. EXPERIMENTAL

2.1 Synthesis

$LiNi_{0.5-x}Zr_xMn_{1.5}O_4$(x= 0.00, 0.03, 0.05, 0.10) samples were synthesized by a combustion synthesis method. The metal nitrates and acetates were used as raw materials with the ratio of 1:1. The fabrication procedure was the same as that employed in our previous works [21, 22]. For convenience, the as-synthesized $LiNi_{0.5-x}Zr_xMn_{1.5}O_4$(x=0.00, 0.03, 0.05, 0.10) were labeled with Zr-0.00, Zr-0.03, Zr-0.05 and Zr-0.10, respectively.

2.2 Characterization

The phase structures and morphologies of Zr-0.00, Zr-0.03, Zr-0.05 and Zr-0.10 were ascertained by XRD (X'pert pro, PANalytical), FT-IR (PerkinElmer, KBr pellets) and SEM (Quanta FEG 250, FEI).

2.3 Electrochemical performance test

The electrochemical performances of the as-synthesized $LiNi_{0.5-x}Zr_xMn_{1.5}O_4$(x=0.00, 0.03, 0.05, 0.10) samples were measured with CR2025 coin cells using a battery system (LAND CT2001A, Wuhan, China) at different C rates (1C=150 mAh/g) between 3.5 V and 5.0 V at 25°C and 55°C. The fabrication procedure of the CR2025 coin cells was the same as that employed in our previous works [21, 22]. Cyclic voltammogram (CV, 3.5V to 5.0V) and electrochemical impedance spectroscopy (EIS, 0.1Hz-100 kHz) recorded on an electrochemical workstation (CHI 660).

3. RESULTS AND DISCUSSION

3.1 Phase composition

The XRD patterns of $LiNi_{0.5-x}Zr_xMn_{1.5}O_4$(x= 0.00, 0.03, 0.05, 0.10) are shown in Fig.1 (a). All peaks of $LiNi_{0.5-x}Zr_xMn_{1.5}O_4$(x= 0.00, 0.03, 0.05, 0.10) correspond to LNMO with well-define cubic spinel structure, which suggestting that the Zr modifying does not obviously influence the structure of

LNMO. In addition, the emergence of many weak peaks corresponds to the ZrO_2 (marked with triangle ▽) when the Zr content is up to 0.05[20, 23]. Usually, LNMO possesses two distinct space groups of the disordered Fd-3m and the ordered $P4_332$ [15]. FT-IR spectroscopy is usually used to differentiate material structure [24]. The FT-IR spectra of $LiNi_{0.5-x}Zr_xMn_{1.5}O_4$(x=0.00, 0.03, 0.05, 0.10) was shown in Fig.1 (b), from which all the products display stronger band intensity at 621 cm^{-1} (Mn-O band) than that at 582 cm^{-1} (Ni-O band), indicating that the as-synthesized $LiNi_{0.5-x}Zr_xMn_{1.5}O_4$(x=0.00, 0.03, 0.05, 0.10) samples possess the more ordered $P4_332$ space groups [8, 25].

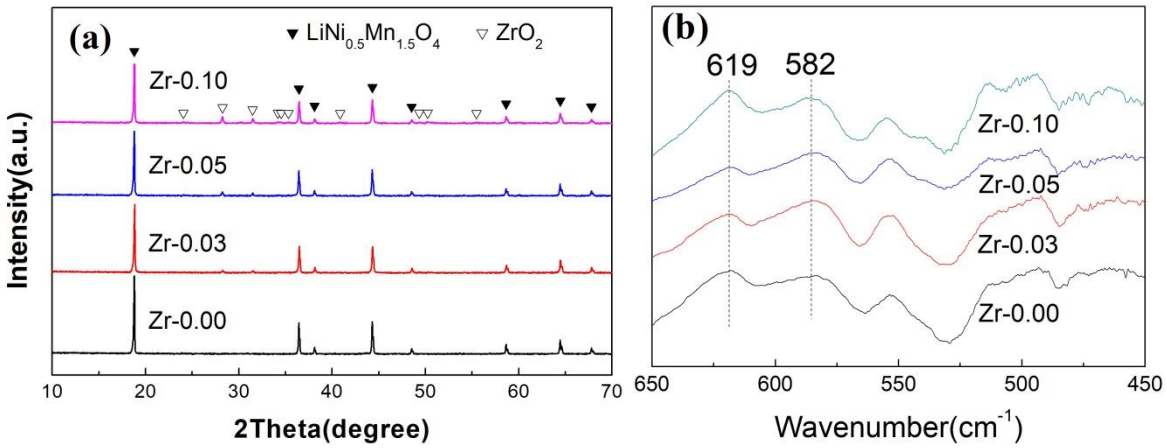

Figure 1. XRD patterns (a) and FT-IR spectra (b) of $LiNi_{0.5-x}Zr_xMn_{1.5}O_4$(x=0.00, 0.03, 0.05, 0.10)

3.2 Morphology

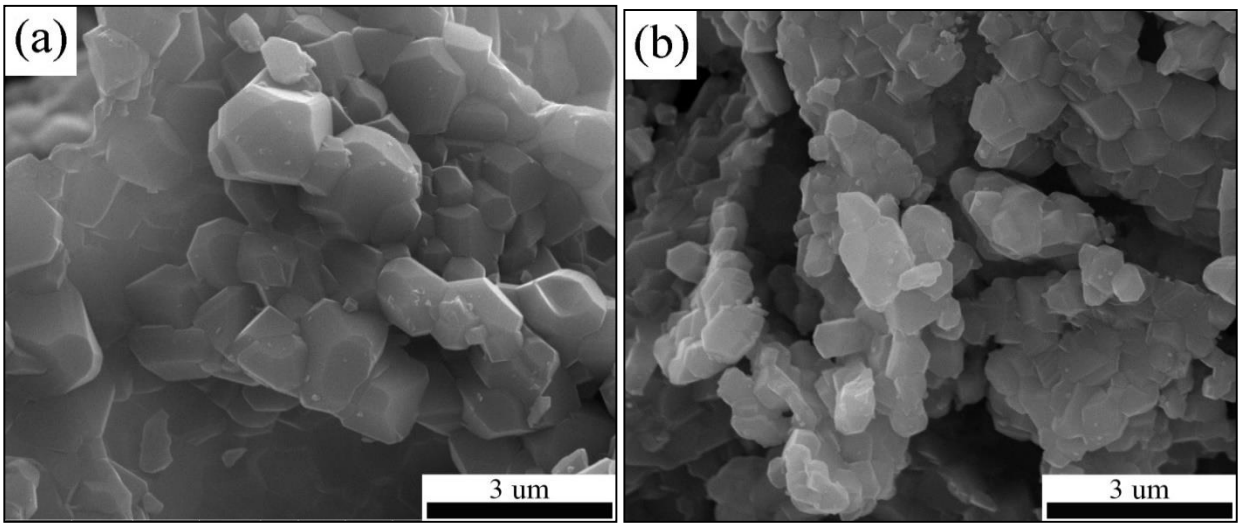

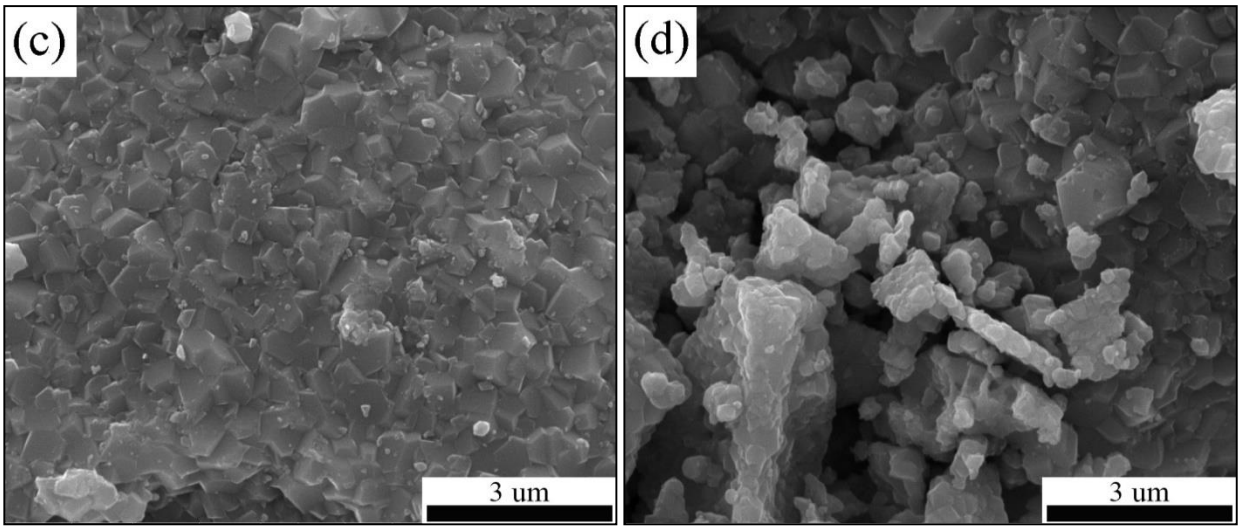

Figure 2. SEM images of $LiNi_{0.5-x}Zr_xMn_{1.5}O_4$ (a-d) (x=0.00, 0.03, 0.05, 0.10)

Fig. 2 (a-d) displays the SEM images of $LiNi_{0.5-x}Zr_xMn_{1.5}O_4$ (x=0.00, 0.03, 0.05, 0.10). The sample without Zr-modifying (Fig. 2(a)) has larger particle sizes than the Zr-modified LNMO samples of Zr-0.03, Zr-0.05 and Zr-0.10 (Fig. 2(b)-Fig. 2(d)). Furthermore, the Zr-0.03, Zr-0.05 and Zr-0.10 present porous morphology and their particle sizes decrease as increasing the Zr content, which is similar as the literature [23].

3.3 Electrochemical performance

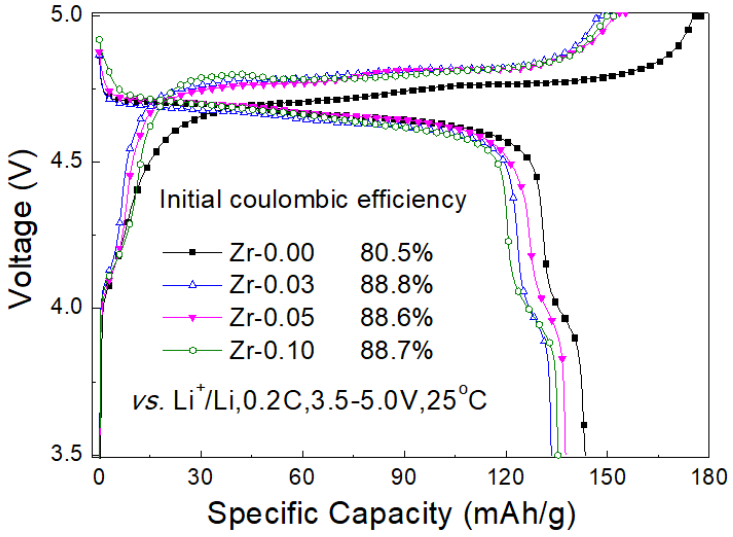

Figure 3. The initial charge-discharge curves of $LiNi_{0.5-x}Zr_xMn_{1.5}O_4$ (x=0.00, 0.03, 0.05, 0.10)

The initial charge-discharge curves of $LiNi_{0.5-x}Zr_xMn_{1.5}O_4$ (x=0.00, 0.03, 0.05, 0.10) are shown in Fig. 3. The discharge curves of $LiNi_{0.5-x}Zr_xMn_{1.5}O_4$ (x=0.00, 0.03, 0.05, 0.10) present two voltage plateaus around at 4.7V and 4.0V, which are assigned the Ni^{2+}/Ni^{4+} and Mn^{3+}/Mn^{4+} redox couples, respectively [5]. The tiny plateau at 4.0V means small amount of Mn^{3+}/Mn^{4+}, implying that the

samples possess high ordering degree, in agreement with the FT-IR results [22, 26]. Compared with the initial coulombic efficiency of Zr-0.00 sample (80.5%), Zr-0.03, Zr-0.05 and Zr-0.10 samples present much higher value of 88.8%, 88.6% and 88.7%, respectively.

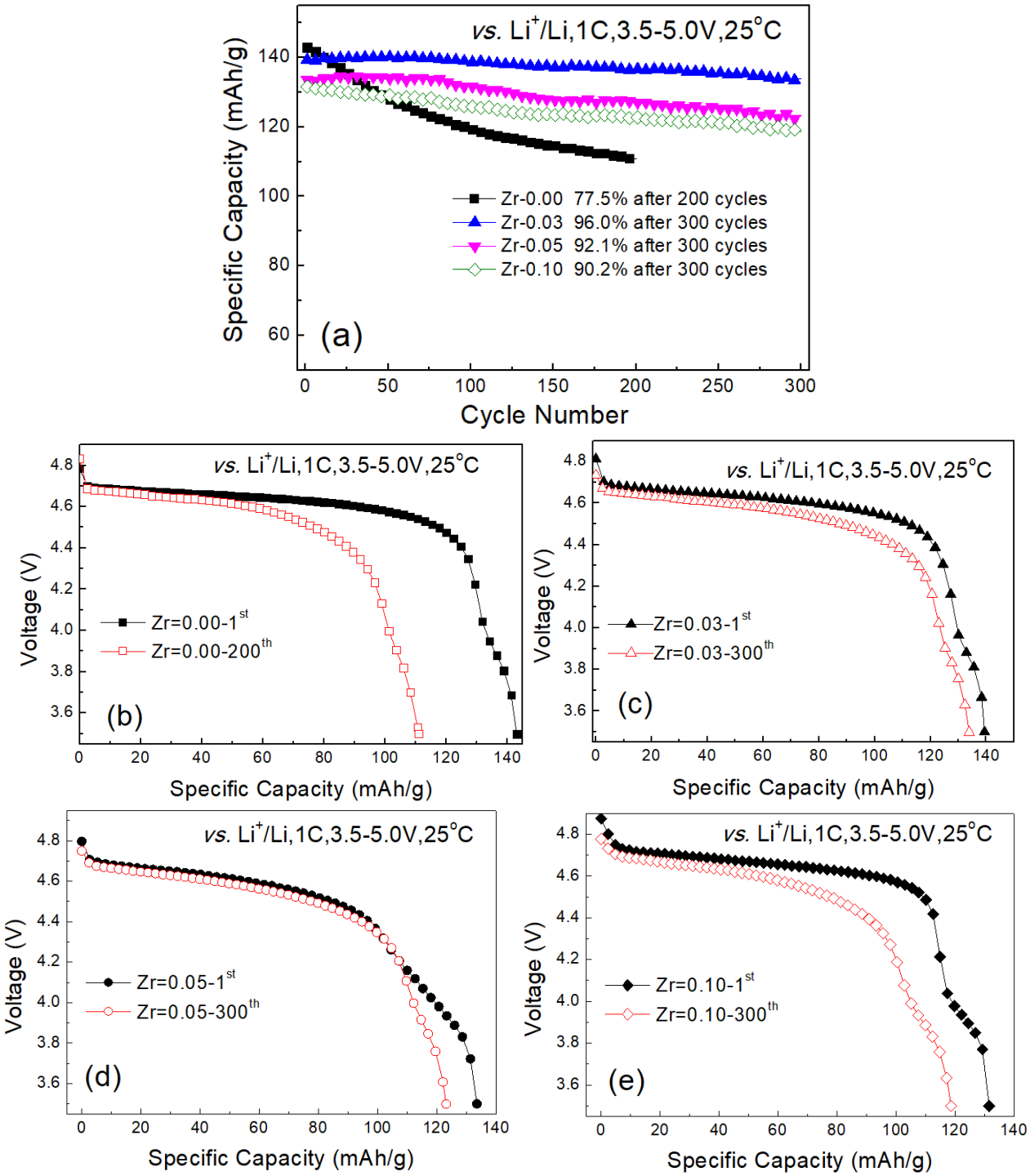

Figure 4. The cycling performance (a) and discharge curves (b-e) of the first and the last cycles of $LiNi_{0.5-x}Zr_xMn_{1.5}O_4$ (x=0.00, 0.03, 0.05, 0.10)

The cyclic performance of $LiNi_{0.5-x}Zr_xMn_{1.5}O_4$ (x=0.00, 0.03, 0.05, 0.10) at 1 C is shown in Fig. 4(a). As is shown in Fig. 4(a), the Zr-0.00 delivers an initial discharge capacity of 143mAh/g at 1C and retains 77.5% of its capacity after 200 cycles. However, the initial specific capacities of Zr-0.03, Zr-0.05 and Zr-0.10 are 139.4, 133.6 and 131.6mAh/g at 1 C, respectively, and they retain 96.0%, 92.1% and 90.2% of their capacities after 300 cycles, respectively. Obviously, Zr-0.03, Zr-0.05 and Zr-0.10 samples present much better cycling performance than that of bare LNMO sample of Zr-0.00. The first and the last discharges of $LiNi_{0.5-x}Zr_xMn_{1.5}O_4$ (x=0.00, 0.03, 0.05, 0.10) at 1C are shown in Fig. 4(b)-Fig. 4(e). The capacity degradation of Zr-0.00 is much faster than those of Zr-0.03, Zr-0.05 and Zr-0.10. Compared with other previous studies, the cycle performance is also excellent [27-29]. The comparison of the cycle performance at 25°C is displayed in Table 1.

Table 1. Comparison of the cycle performance at 25°C

Samples	The capacity retention/%	Conditions	Literatures
$LiNi_{0.47}Zr_{0.03}Mn_{1.5}O_4$	96.0	1C, 300th cycle	This work
$LiNi_{0.5}Mn_{1.5}O_4$	85.2	0.5C, 100th cycle	[27]
$LiNi_{0.5}Mn_{1.5}O_4$	81.33	0.2C, 100th cycle	[28]
$LiNi_{0.5}Mn_{0.485}Si_{0.015}O_2$	78	1C, 100th cycle	[29]

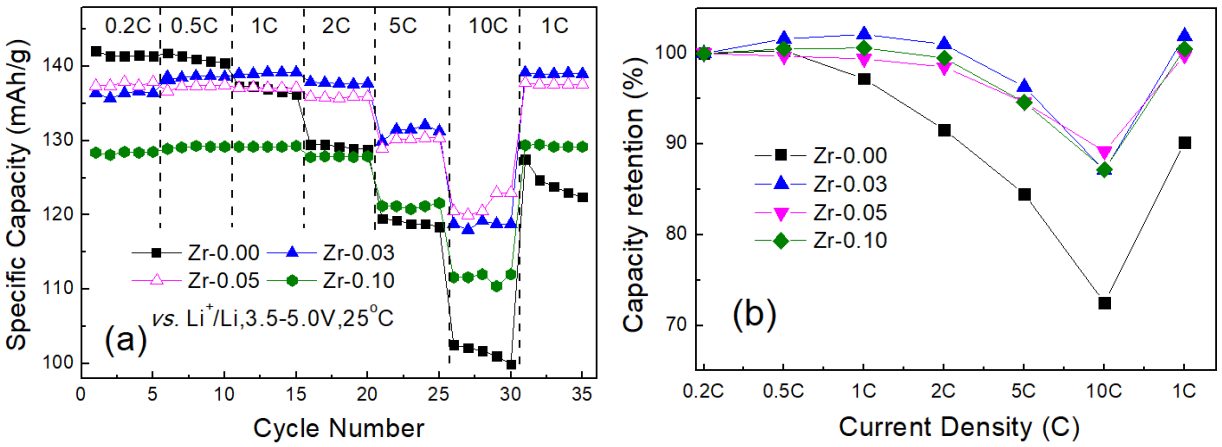

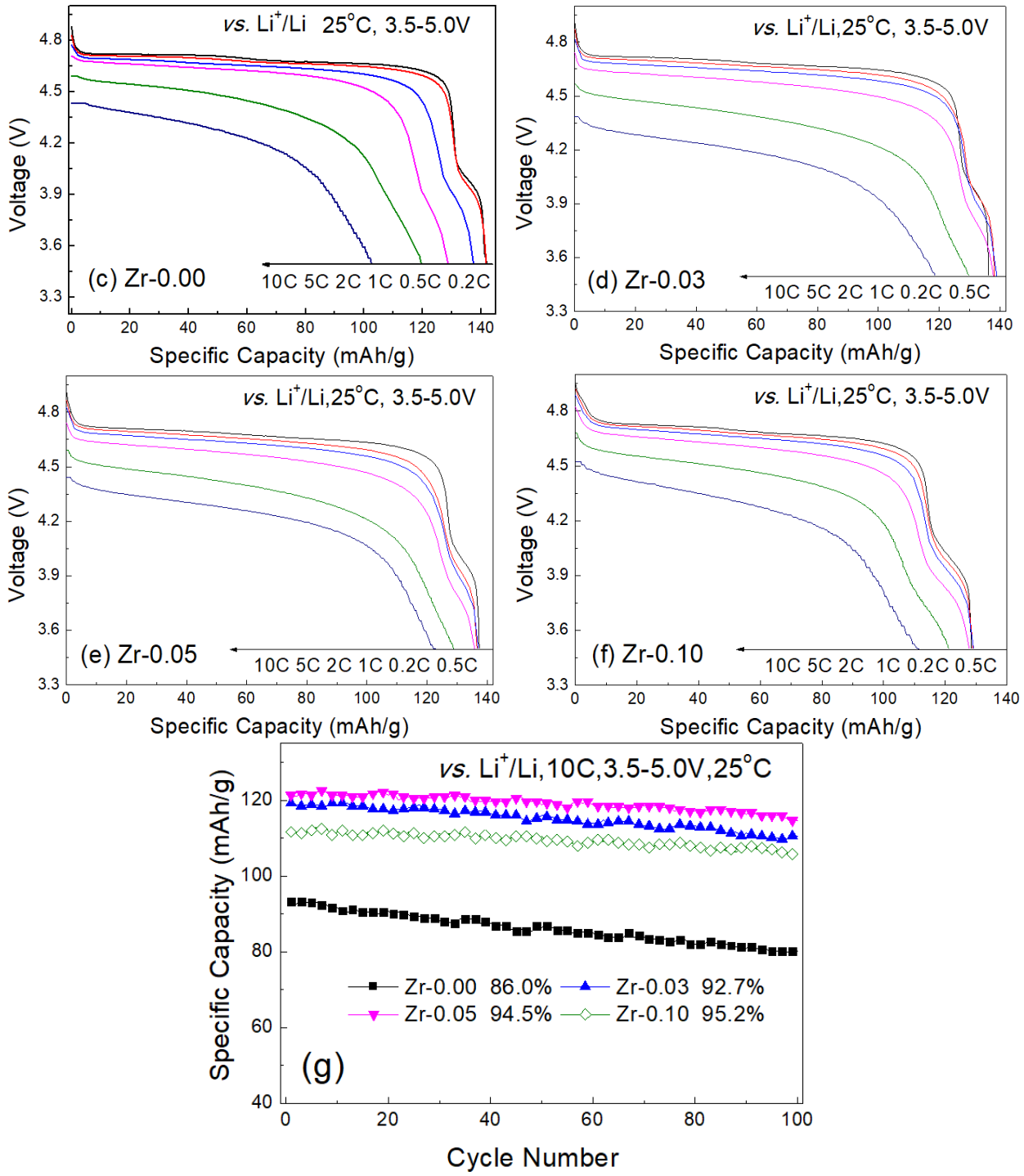

Figure 5. The rate capability (a), capacity retentions (b), discharge curves (c-f) at different rate and cycle performance (g) at 10C of $LiNi_{0.5-x}Zr_xMn_{1.5}O_4$ (x=0.00, 0.03, 0.05, 0.10) at 25°C

The rate capability of $LiNi_{0.5-x}Zr_xMn_{1.5}O_4$ (x=0.00, 0.03, 0.05, 0.10) is shown in Fig.5 (a) and Fig.5 (b). Zr-0.03, Zr-0.05 and Zr-0.10 samples present more excellent rate capability than bare LNMO sample of Zr-0.00, especially at 10C rate. Fig.5 (c)-Fig.5 (f) display $LiNi_{0.5-x}Zr_xMn_{1.5}O_4$ (x=0.00, 0.03, 0.05, 0.10) discharge curves at different rate, from which the rate capability of LNMO is enhanced after Zr modifying. At 10C, the capacity retention of Zr-0.03, Zr-0.05 and Zr-0.10 is 92.7%, 94.5% and 95.2%, respectively, much higher than the 86.0% of Zr-0.00 after 100 cycles (as shown in

Fig. 5(g)). Moreover, Zr-modified LNMO samples show much better rate capabilities and high-rate cycle performance than documents [16, 29, 30]. The comparison of the discharge capacity at 10 C is summarized in Table 2.

Table 2. Comparison of the discharge capacity at 10 C

Samples	Discharge specific capacity (mAh/g)	Conditions	Literatures
$LiNi_{0.4}Zr_{0.1}Mn_{1.5}O_4$	121.3	10C, 95.2%, 100^{th}cycle	This work
$LiNi_{0.5}Mn_{1.45}Si_{0.05}O_4$	100	10C	[16]
$LiNi_{0.5}Mn_{0.485}Si_{0.015}O_2$	75	10C	[29]
$LiNi_{0.5}Mn_{1.5}O_4$	0	10C	[30]

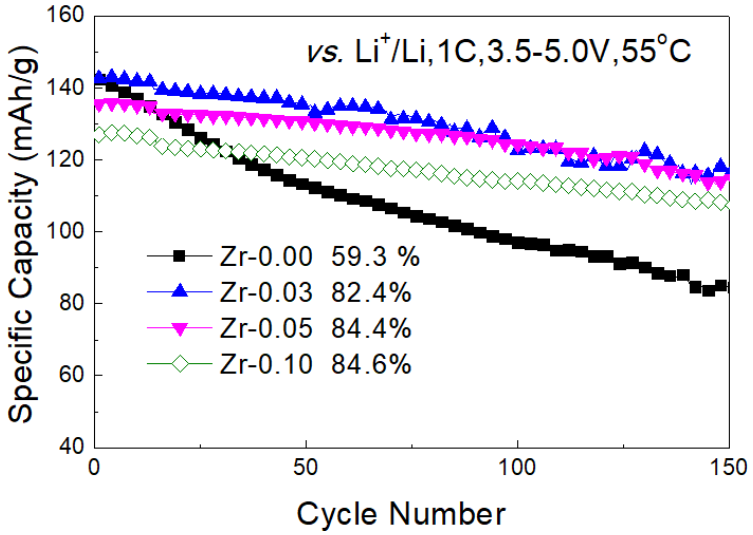

Figure 6. Cycle performance of $LiNi_{0.5-x}Zr_xMn_{1.5}O_4$ (x=0.00, 0.03, 0.05, 0.10) at 55°C

The thermal stability of materials directly related to the battery safety at elevated temperatures [24]. Fig. 6 shows the cycle performance of $LiNi_{0.5-x}Zr_xMn_{1.5}O_4$ (x= 0.00, 0.03, 0.05, 0.10) at 1C rate at 55°C. The specific capacities of Zr-0.00, Zr-0.03, Zr-0.05 and Zr-0.10 are 84.6, 117.6, 114.5, and 107.4mAh/g, respectively, and they retain 59.3%, 82.4%, 84.4%, and 84.6% of their capacities after 150 cycles at 55°C, respectively. Obviously, the cycle performance of LNMO was improved significantly after Zr modifying at elevated temperature (55°C).

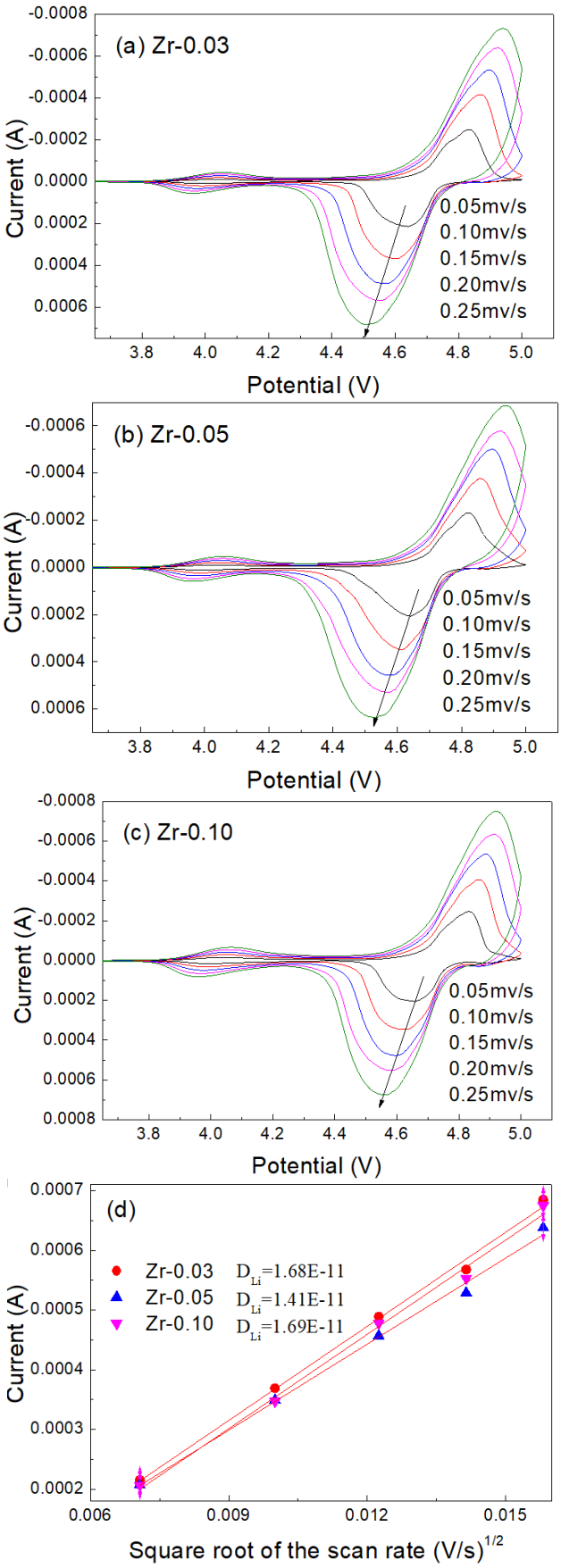

Figure 7. CV of $LiNi_{0.5-x}Zr_xMn_{1.5}O_4$ (x= 0.03, 0.05, 0.10) (a-c) at various scan rates and the plotting of peak current (i_p) vs. square root of the scan rate ($v^{1/2}$) (d)

To understand electrochemical behavior of Zr-0.03, Zr-0.05 and Zr-0.10, cyclic voltammetry (CV) was performed at 0.05-0.25mv/s. The peaks around at 4.7V with broadened shapes and 4.0V with low intensity correspond to the Ni^{2+}/Ni^{4+} and Mn^{3+}/Mn^{4+} redox couples, respectively, as is shown in Fig. 7(a)-Fig. 7(c). The results suggest that Zr-0.03, Zr-0.05 and Zr-0.10 contain few Mn^{3+} ions and maintain high ordering degree, consistent with the results of FT-IR and the discharge-curve above. In addition, CV aslo can be used to envalue the diffusion coefficient of Li^+ (D_{Li}) [31]. Fig. 7(d) plots i_p vs. $v^{1/2}$ of Zr-0.03, Zr-0.05 and Zr-0.10 at 0.05-0.25 mV/s, which calculated D_{Li} values are $1.68\times10^{-11}cm^2/s$, $1.41\times10^{-11}cm^2/s$ and $1.69\times10^{-11}cm^2/s$, respectively, resulting in the excellent rate capabilities.

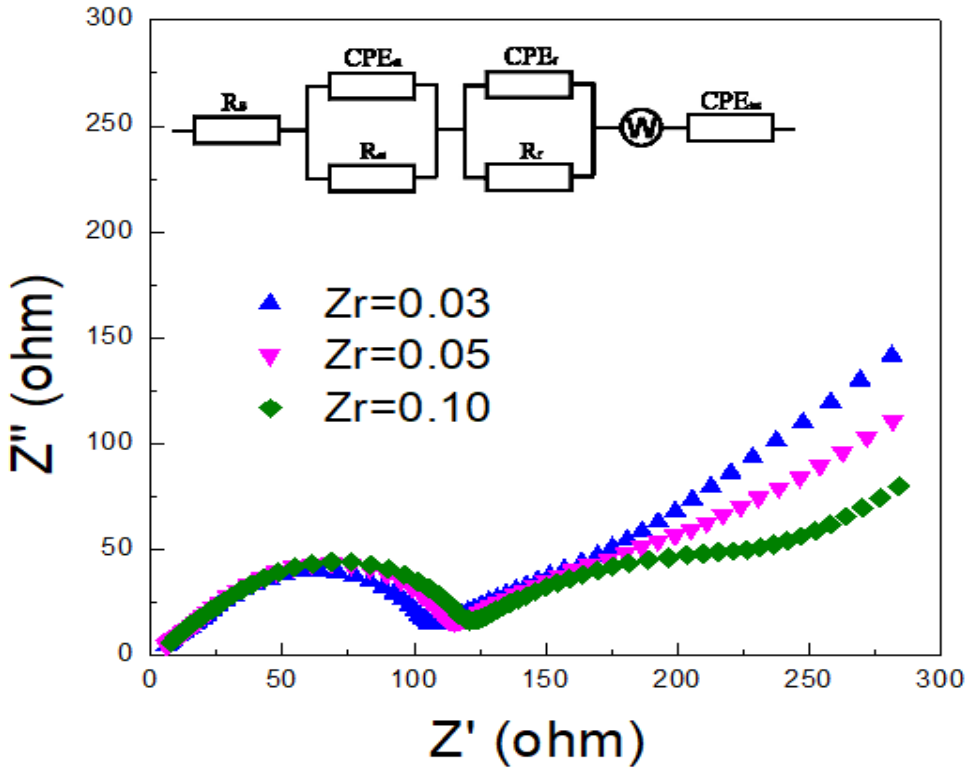

Figure 8. EIS spectra of $LiNi_{0.5-x}Zr_xMn_{1.5}O_4$ (x= 0.03, 0.05, 0.10) in the frequency range from 0.1Hz to 100 kHz after 3rd cycles

The EIS of $LiNi_{0.5-x}Zr_xMn_{1.5}O_4$ (x=0.03, 0.05, 0.10) after 3rd cycles and a possible equivalent circuit are shown in Fig. 8, from which the charge transfer resistance (Rct) of Zr-modified Zr-0.03, Zr-0.05 and Zr-0.10 has no obvious chang and is higher than those of prime LNMO prepared by other methods, resulting in the excellent rate capability [32].

4. CONCLUSIONS

$LiNi_{0.5-x}Zr_xMn_{1.5}O_4$ (x=0.00, 0.03, 0.05, 0.10) samples were successfully prepared by a combustion synthesis method. All the samples were mainly composed of ordered $P4_332$ space group

and formed ZrO_2 impurity when the Zr content reaches 0.05. The Zr-modified LNMO samples present porous morphology and had smaller particle sizes than bare LNMO. The rate capability and cycle performance of the LNMO samples both at 25°C and 55°C are significantly improved after Zr-modifing. Zr-modified samples of Zr-0.03, Zr-0.05 and Zr-0.10 retain 96.0%, 92.1% and 90.2% of their capacities after 300 cycles at 25°C, respectively，whereas bare LNMO only retains 77.5%. Meanwhile, the capacity retentions of Zr-0.03, Zr-0.05 and Zr-0.10 after 150 cycles at elevated temperature (55°C) are 82.4%, 84.4% and 84.6%, respectively, which are higher than 59.3% of bare LNMO. Furthermore, the capacity retention of Zr-modified samples of Zr-0.03, Zr-0.05 and Zr-0.10 are over 92% after 100 cycles at 10C.

ACKNOWLEDGEMENT
This work was supported by the National Natural Science Foundation of China (No. 51662007 and No. U1602273), the Honghe University Research Project (SZ1822) and the Key Construction Disciplines of Chemistry for Master Degree Program in Yunnan.

References

1. Y. Luo, T. Lu, Y. Zhang, L. Yan, S.S. Mao, J. Xie, *J. Alloys Compd.,* 703 (2017) 289-297.
2. Y. Yao, H. Liu, G. Li, H. Peng, K. Chen, *Mater. Chem. Phys.,* 143 (2014) 867-872.
3. J.H. Kim, N.P.W. Pieczonka, Z. Li, Y. Wu, S. Harris, B.R. Powell, *Electrochim. Acta*, 90 (2013) 556-562.
4. T.F. Yi, X. Han, B. Chen, Y.R. Zhu, Y. Xie, *J. Alloys Compd.*, 703 (2017) 103-113.
5. S.P. Feng, X. Kong, H.Y. Sun, B.S. Wang, H. Yin, G.Y. Liu, *Int. J. Electrochem. Sci.*, 13 (2018) 4276-4284.
6. J. Chong, S. Xun, X. Song, G. Liu, V.S. Battaglia, *Nano Energy*, 2 (2013) 283-293.
7. T.F. Yi, Y.M. Li, X.Y. Li, J.J. Pan, Q. Zhang, Y.R. Zhu, *Sci. Bull.*, 62 (2017) 1004-1010.
8. W. Liu, Q. Shi, Q. Qu, T. Gao, G. Zhu, J. Shao, H. Zheng, *J. Mater. Chem. A*, 5 (2017) 145-154.
9. W. Wu, J. Guo, X. Qin, C. Bi, J. Wang, L. Wang, G. Liang, *J. Alloys Compd.,* 721 (2017) 721-730.
10. J. Wang, W. Lin, B. Wu, J. Zhao, *Electrochim. Acta*, 145 (2014) 245-253.
11. O. Sha, Z. Qiao, S. Wang, Z. Tang, H. Wang, X. Zhang, Q. Xu, *Mater. Res. Bull.*, 48 (2013) 1606-1611.
12. H. Sun, X. Kong, B. Wang, T. Luo, G. Liu, *Int. J. Electrochem. Sci.*, 12 (2017) 8609-8621.
13. X. Liu, D. Li, Q. Mo, X. Guo, X. Yang, G. Chen, S. Zhong, *J. Alloys Compd.,* 609 (2014) 54-59.
14. J. Mao, M. Ma, P. Liu, J. Hu, G. Shao, V. Battaglia, K. Dai, G. Liu, *Solid State Ionics,* 292 (2016) 70-74.
15. G. Liu, J. Zhang, X. Zhang, Y. Du, K. Zhang, G. Li, H. Yu, C. Li, Z. Li, Q. Sun, L. Wen, *J. Alloys Compd.,* 725 (2017) 580-586.
16. S. Nageswaran, M. Keppeler, S.-J. Kim, M. Srinivasan, *J. Power Sources*, 346 (2017) 89-96.
17. M. Mo, K.S. Hui, X. Hong, J. Guo, C. Ye, A. Li, N. Hu, Z. Huang, J. Jiang, J. Liang, H. Chen, *Appl. Surf. Sci.*, 290 (2014) 412-418.
18. H. Wang, H. Xia, M.O. Lai, L. Lu, *Electrochem. Commun.*, 11 (2009) 1539-1542.
19. T.F. Yi, Y. Xie, Y.R. Zhu, R.S. Zhu, M.F. Ye, *J. Power Sources*, 211 (2012) 59-65.
20. J. Yoon, M. Jeong, I.T. Bae, K.-W. Nam, W.-S. Yoon, *J. Power Sources*, 368 (2017) 1-10.
21. S.P. Feng, X. Kong, H. Sun, B. Wang, T. Luo, G. Liu, *J. Alloys Compd.,* 749 (2018) 1009-1018.
22. H.Y. Sun, X. Kong, B.S. Wang, T.B. Luo, G.Y. Liu, *Ceram. Int.*, 44 (2018) 4603-4610.
23. X. Li, M. Qu, Z. Yu, *J. Alloys Compd.,* 487 (2009) L12-L17.

24. L. Wang, D. Chen, J. Wang, G. Liu, W. Wu, G. Liang, *Powder Technol.*, 292 (2016) 203-209.
25. X. Kong, H. Sun, Z. Yi, B. Wang, G. Zhang, G. Liu, *Materials Technology*, (2016) 1-7.
26. J. Yang, X. Han, X. Zhang, F. Cheng, J. Chen, *Nano Res.*, 6 (2013) 679-687.
27. E. Zhao, L. Wei, Y. Guo, Y. Xu, W. Yan, D. Sun, Y. Jin, *J. Alloys Compd.,* 695 (2017) 3393-3401.
28. Y.L. He, J. Zhang, Q. Li, Y. Hao, J.W. Yang, L.Z. Zhang, C.L. Wang, *J. Alloys Compd.,* 715 (2017) 304-310.
29. J.K. Chen, X.H. Tan, H.Q. Liu, L.M. Guo, J.T. Zhang, Y. Jiang, J. Zhang, H.F. Wang, X.M. Feng, W.G. Chu. *Electrochim. Acta*, 228 (2017) 167-174.
30. T. Kozawa, T. Murakami, M. Naito, *J. Power Sources*, 320 (2016) 120-126.
31. F. Fu, Y. Yao, H. Wang, G.L. Xu, K. Amine, S.G. Sun, M. Shao, *Nano Energy*, 35 (2017) 370-378.
32. J. Liu, A. Manthiram, *J. Phys. Chem. C,* 113 (2009) 15073-15079.